



Original Research

Mesh Convergence Study of Three-Dimensional Femoral Bone and Stem Models: A Finite Element Method

Nik Nur Ain Azrin Abdullah¹, Muhammad Hanif Baharuddin¹, Aishah Umairah Abd Aziz¹, Nur Afikah Zainal Abidin¹, Gan Hong Seng², Mohammed Rafiq Abdul Kadir³, Muhammad Hanif Ramlee^{1,4*}

¹Bone Biomechanics Laboratory (BBL), Department of Biomedical Engineering and Health Sciences, Faculty of Electrical Engineering, Universiti Teknologi Malaysia, Johor Bahru, 81310, Johor, Malaysia

²School of AI and Advanced Computing, XJTLU Entrepreneur College (Taicang), Xi'an Jiatong-Liverpool University, Suzhou, 215400 China

³Department of Biomedical Engineering, Faculty of Engineering, Universiti Malaya, Kuala Lumpur 50603, Federal Territory of Kuala Lumpur, Malaysia

⁴Rehabilitation Nexus (RehabNex) Research Group, Health and Wellness Research Alliance, Universiti Teknologi Malaysia, Johor Bahru 81310, Johor, Malaysia

ARTICLE INFO

Article History:

Received 29 May 2025

Accepted 1 August 2025

Available online 1 August 2025

Keywords:

Mesh convergence study;
Finite element analysis (FEA);
Femoral bone;
Femoral stem;

ABSTRACT

The demand for total hip arthroplasty (THA) surgery is projected to rise annually, as indicated by analysis of past surgical data. The researchers consistently strive to enhance the hip implant design, responding to the growing demand that has evolved from solid implant designs to advanced porous implants. A widely utilized approach involves the application of finite element analysis (FEA) to the design of hip implants, as it significantly reduces both time and costs in comparison to conventional physical testing methods. However, it is essential to determine the appropriate mesh size prior to conducting FEA to ensure that it doesn't affect the reliability of the results. Hence, the objective of this study is to conduct a mesh convergence analysis of the femoral bone and stem. This study involved the reconstruction of the femoral bone and the development of the femoral stem utilizing Mimics and SolidWorks software. The h-refinement method and analysis were conducted using the 3-Matic and MSC Marc Mentat software, with a mesh size range of 6.0 mm to 3.5 mm for the femoral bone and 4.0 mm to 2.0 mm for the femoral stem. According to results, the optimal mesh size for the femoral bone and femoral stem was 4.5 mm and 3.0 mm, respectively. The mesh convergence analysis for this study was successfully conducted, with the percentage error between two successive models demonstrated to be less than 5%.

INTRODUCTION

Total hip arthroplasty (THA) is a surgical procedure that involves the replacement of a compromised hip joint with an artificial implant (prosthesis). THA is expected to increase around 284% (to a predicted yearly volume of 1.43 million surgeries) by 2040, according to an analysis by Singh et al. based on data from the Census Bureau and the U.S. National Inpatient Sample (NIS) from 2000 to 2014 (Singh et al., 2019).

Furthermore, a rising trend of 659% has been reported by 2060%, according to the Centers for Medicare & Medicaid Services (CMS) Medicare/Medicaid Part B National Summary data (Shichman et al., 2023). The escalating incidence of THA surgeries has prompted researchers to expand their focus on the improvement of hip implant design. This work involves enhancements to vital components such as the femoral stem, acetabular cup, and femoral head (ball), with the purpose of improving performance, lifespan, and patient outcomes (Borah et al., 2021).

Over the past few years, there have been numerous methods by which researchers and developers have enhanced the design of solid hip implants. Nonetheless, the stress shielding

* Muhammad Hanif Ramlee (muhammad.hanif.ramlee@biomedical.utm.my)

Rehabilitation Nexus (RehabNex) Research Group, Health and Wellness Research Alliance, Universiti Teknologi Malaysia, Johor Bahru 81310, Johor, Malaysia

phenomenon is one of the current issues. This phenomenon arises as a result of the increased rigidity of the current materials used in solid hip implants, which include titanium, cobalt chromium, and stainless steel (Choroszyński et al., 2017). The imbalance of load transfer occurs when the solid implant is inserted into the femur, as the majority of the load is distributed to the implant rather than the surrounding bone (Arabnejad et al., 2017). As a result, this can lead to serious issues such as fractures, thigh soreness, and, in the worst-case scenario, a second surgery (Abdullah et al., 2025; Prasad et al., 2017). Hence, it is recommended that the implant incorporate a porous/lattice design to mitigate the aforementioned issue. Currently, the majority of researchers design porous hip implants by employing finite element analysis (FEA).

FEA is a computerized technique that is employed to forecast the behavior of a product or model in response to real-world forces (Fish et al., 2007). This method is more efficient in terms of time and cost, as it does not necessitate physical testing. Numerous research studies have employed FEA in the development of porous hip implants; for instance, Kladovasilakis et al. analyzed various lattice structures (Voronoi, Gyroid, and Schwarz Diamond) using FEA under static in vivo loadings (Kladovasilakis et al., 2020). The FEA for each implant aims to ascertain its yield point and safety factor. A tetrahedral mesh and the nickel-based superalloy Inconel 718 material were utilized in this study. In another study, Cheah et al. conducted a static finite-element analysis on Ti-6Al-4V hip implants with lattice structures (Cubic FBCCZ and Octet-truss) that varied in density (Cheah et al., 2022). The mesh sizes were selected to be three times smaller than the strut thickness to ensure sufficient computational requirements, time efficiency, and precision.

Previous research has shown that mesh generation is one of the parameters that need to be identified before FEA can be conducted. It is imperative to ascertain the appropriate mesh size, as the quality of the mesh is a significant factor in the computational efficiency, accuracy, and reliability of FEA results. In general, a finer mesh will produce more accurate results; nevertheless, it will also require a lot more time and resources to compute (Mohamad Azmi et al., 2024). Hence, a mesh convergence study is indispensable for the purpose of determining the optimal mesh size. Therefore, the objective of this study is to conduct a mesh convergence analysis of the femoral bone and stem to prevent the simulation results from being influenced by the variability of mesh size.

MATERIALS AND METHOD

Reconstruction and Development of 3D Femoral Bone and Stem

For the reconstruction of the femoral bone, the data used in this study were derived from computed tomography (CT) scans of a 27-year-old male subject who weighed 75 kg and measured at a height of 169 cm. The scans were obtained at Hospital Tengku Ampuan Afzan in Kuantan, Pahang, Malaysia (no: versi2.0tarikh15Feb2008) (Abd Aziz et al., 2024). Firstly, the CT dataset was imported into Mimics software (Materialise, Leuven, Belgium) to create a precise three-dimensional (3D) model of the femur bone. Bone segmentation was executed with a specified Hounsfield Unit (HU) threshold range of 226 to 3071

HU. The “Region Grow” and “Split Mask” tools were utilized to delineate the right femur bone and remove extraneous adjacent bone components. After the segmentation process, the “Calculate” function was employed to construct the 2D image segments into a 3D model. The femur bone model was exported as a stereolithography (STL) file and then imported into 3-Matic software (Materialise, Leuven, Belgium) for mesh production. Figure 1 below shows a visual representation of the stages involved in femur bone reconstruction. For the development of the femoral stem, SolidWorks (Dassault Systèmes, Vélizy-Villacoublay, France) software was employed to mimic the commercial hip implant design, which originates from the Taperloc by Zimmer Biomet. The supplier’s specifications in the brochure or catalogue were used to establish the implant’s dimensions, and the length of the stem was fixed at 160 mm in accordance with previous studies (Delikanli et al., 2019; Kladovasilakis et al., 2020).

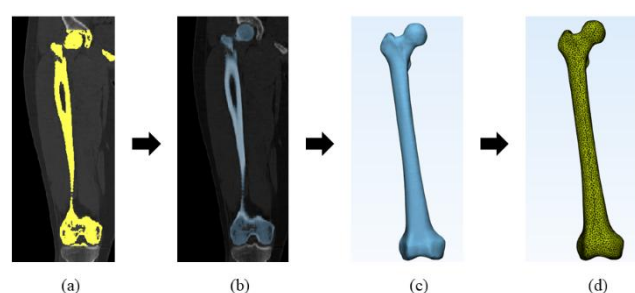


Fig. 1 Reconstruction process of the 3D femoral bone: (a) auto-segmentation model, (b) manual segmentation model, (c) conversion from a 2D to 3D model, (d) mesh production

Convergence Analysis

The 3-Matic software (Materialise, Leuven, Belgium) has been employed to create a mesh of the femoral bone and stem using a 3D triangular surface mesh, also referred to as a tetrahedral mesh. Next, the convergence study of the femoral bone and stem began with the refining method. Refinement is a remesh process that separates a triangular mesh into defined sizes; in this investigation, h-refinement was used. The femoral bone was composed of six distinct mesh densities, with sizes ranging from 6.0 mm to 3.5 mm (Figure 2), while the femoral stem was composed of five distinct mesh densities, with sizes ranging from 4.0 mm to 2.0 mm (Figure 3). Table 1 displays the number of nodes and elements for each model with a variation in mesh size. Following this, the models were converted to solid tetrahedral using the 3-Matic software, exported as an STL file, and integrated into the MSC Marc Mentat software (MSC.Software Corporation, Germany) for analysis. The FEA was performed on each model with all parameters, including material properties and boundary conditions, remaining consistent. The Young’s modulus and Poisson ratio for bone material were set to 7 GPa and 0.3, whereas stem material (titanium alloy) were set to 114 GPa and 0.31. For boundary conditions, the proximal femoral bone and stem were subjected to a 375 N axial load to replicate the standing phase of the human gait cycle (Figure 4). After the study was concluded, the von Mises stress (VMS) data was obtained by selecting a single node for each model.

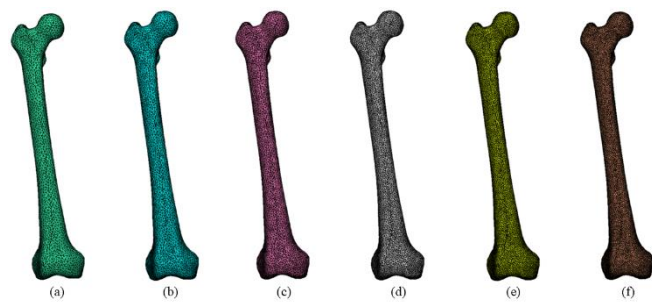


Fig. 2 Six mesh size of femoral bone: (a) 6.0 mm, (b) 5.5 mm, (c) 5.0 mm, (d) 4.5 mm, (e) 4.0 mm, (f) 3.5 mm

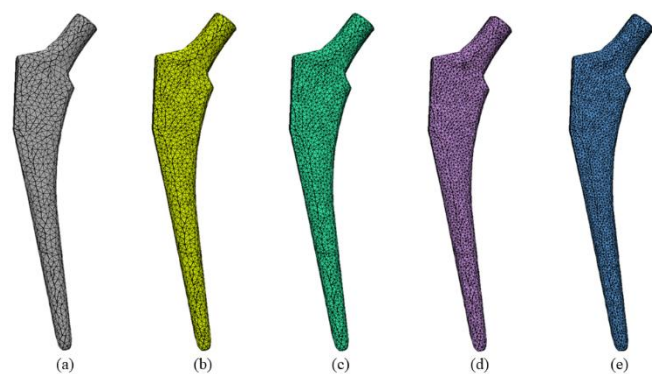


Fig. 3 Five mesh size of femoral stem: (a) 4.0 mm, (b) 3.5 mm, (c) 3.0 mm, (d) 2.5 mm, (e) 2.0 mm

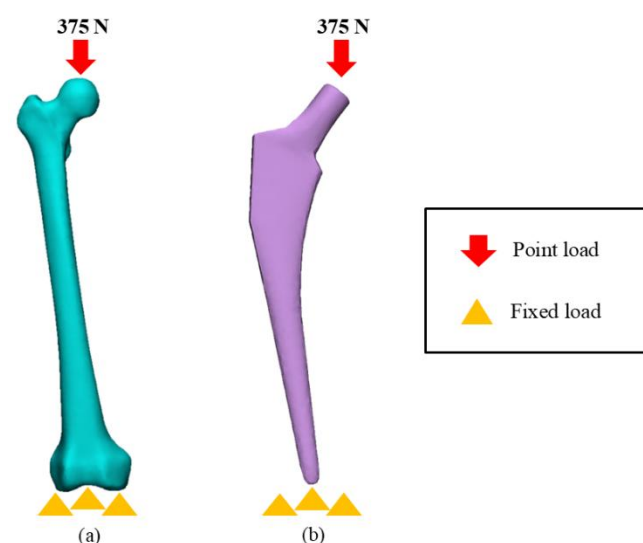


Fig. 4 Boundary conditions for convergence analysis: (a) femoral bone model, (b) femoral stem model

RESULT AND DISCUSSION

In order to conduct the convergence analysis, the triangular meshes of the models were refined and subdivided using the 4-node tetrahedral element, which has been demonstrated to be more precise than its corresponding element (Mughal et al., 2015). Besides that, mesh convergence was performed separately for the implant and the femoral bone due to differences in mesh sensitivity arising from their distinct material properties and geometric complexities. This approach also ensures that each component achieves solution accuracy efficiently prior to assembly and contact analysis. The methodology is supported by recent biomechanical FEA studies. For example, Gok (2022) refined the implant mesh to approximately 0.5 mm and the bone mesh to around 3 mm, meeting convergence criteria with less than 5% variation in stress and displacement. Similarly, a study by Bilgi-Ozyetim et al. (2025) conducted independent mesh refinement for the implant and bone, achieving a relative error of less than 2–3% in stress values.

Moreover, the h-refinement method was implemented in this convergence study, as it has the potential to improve finite element results by employing a smaller mesh size (De Sterck et al., 2008). The bone's mesh sizes varied from 6.0 mm to 3.5 mm, whereas the stem's range was 4.0 mm to 2.0 mm. The mesh size range in this study was selected based on the maximum and minimum values reported in previous literature. For instance, a study by Salaha et al. (2023) utilized a femoral mesh ranging from 6 mm to 3.5 mm, reporting no significant variation in results below these thresholds. For implants, most studies employed a mesh size of approximately 3 mm; therefore, a range of 4 mm to 2 mm was selected for the implant in this study (Alkhatib et al., 2019; Trentadue et al., 2023). The use of a 0.5 mm decrement ensures adequate resolution for convergence assessment while remaining consistent with mesh sensitivity limits reported in the literature for both bone and implant models.

In addition, the models were subjected to a compressive load of half the body weight (375 N) to replicate a standing leg state. The distal section of the models was fixed using the MSC Marc Mentat software (Ramlee et al., 2014). As shown in Figure 5, the VMS value was acquired at the same place in every model after the analysis. A single node at a consistent coordinate was selected and evaluated in all simulations to ensure reliable convergence assessment. This method reduces variability caused by differing evaluation points and allows for direct comparison of mesh refinement effects on localized mechanical responses. The practice of using a fixed node location is well established in finite element analysis, as outlined by Cook et al. (2002) and Zienkiewicz et al. (2013). To facilitate comparison, graphs were drawn using the VMS data versus the number of elements.

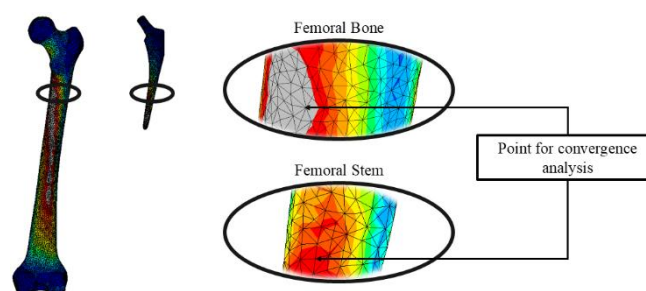
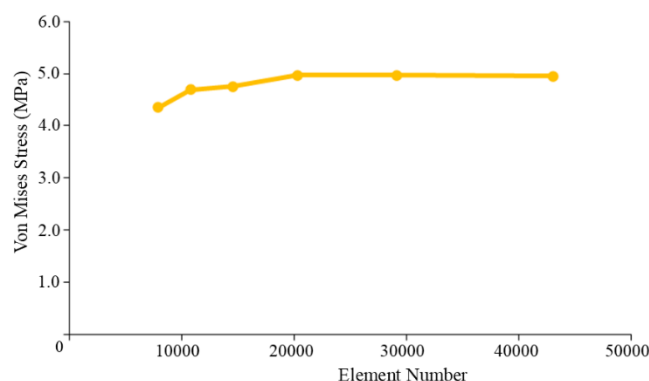
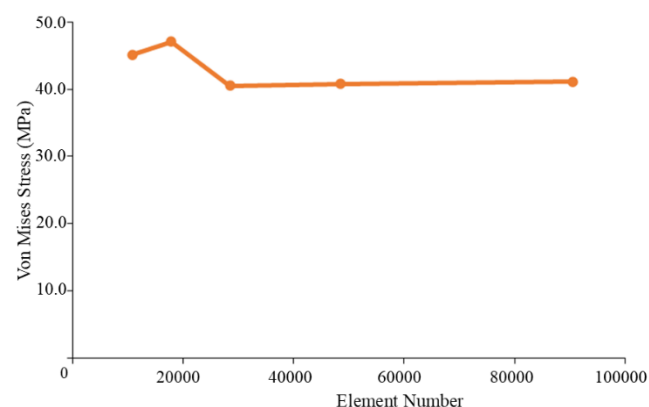
In Figure 6, the von Mises stress distribution for the femoral bone increased with the number of elements and stabilized around the fourth iteration (202916 elements). The stress distribution of the femoral bone observed in this study is almost similar with that reported by Salaha et al. (2023) when evaluated at the same node, with values ranging between 2 and 4 MPa. Next, the percentage error between two successive models was

Table 1 Number of nodes and elements for both models with a variation in mesh size

FE Model	Mesh Size (mm)	Number of Elements	Number of Nodes
Femoral bone	6.0	78994	14584
	5.5	107766	19873
	5.0	145346	26664
	4.5	202916	36967
	4.0	290732	52096
	3.5	430595	75672
Femoral stem	4.0	10832	2433
	3.5	17877	5068
	3.0	28475	8907
	2.5	48522	15665
	2.0	90495	28602

calculated to determine the convergence point. The percentage differences calculated from model 1 (78994 elements) to model 4 (202916 elements) were 7.47%, 1.41%, and 4.35%. From model 4 (202916 elements) to model 6 (430595 elements), the percentage differences were 0.07% and 0.45%. Given that the values between model 4 and model 6 were below 5%, the model was deemed to have converged at that point (Chen et al., 2014; Ramlee et al., 2018; Spirka et al., 2014). The graph presented in Figure 6 supports this assumption, indicating that convergence initiates at model 4, which comprises 202916 elements. Therefore, model 4 (4.5 mm) was identified as the optimal mesh size for this study, aligning with findings from prior research (Salaha et al., 2023). Most previous studies utilized a mesh size of 4 mm, differing by 0.5 mm from the current study; however, this mesh size remains within the acceptable range, as it varies according to the model used (Jetté et al., 2018; Kim et al., 2019).

In contrast to the prior graph, the stress distribution for the femoral stem decreased as the number of elements increased until it remained nearly constant by the third attempt (28475 elements). The stress distribution of the femoral stem obtained in this study under a 375 N load, with a peak von Mises stress of approximately 40 MPa, shows reasonable agreement with the findings of Guzmán et al. (2022), where a 2300 N load resulted in a peak stress of around 200 MPa. Although the loading magnitudes and boundary conditions differ, the stress values scale proportionally, thereby supporting the validity of our simulation results. Besides that, the percentage difference calculated from model 1 (10832 elements) to model 3 (28475 elements) was 4.21% and 14.93%. From model 3 (28475 elements) to model 5 (90495 elements), the percentage difference was 0.65% and 0.84%. Consequently, models 3 to 5 were selected based on a convergence criterion of less than 5%, as validated by the graph in Figure 7, which indicates that convergence begins at model 3 (28475 elements). Consistent with prior research (Alkhatib et al., 2019), this study used model 3 (3.0 mm) as the ideal mesh size for the femoral stem. Despite the differing patterns exhibited by both graphs, their validity is supported by previous literature (Tafreshi et al., 2019; Yaman et al., 2015).

**Fig. 5** The node location for each model in convergence analysis**Fig. 6** Convergence study graph for femoral bone**Fig. 7** Convergence study graph for femoral stem

CONCLUSION

In summary, the research successfully conducted mesh convergence analysis for both the femoral bone and stem using the h-refinement method and a simple analysis setup for each model. The analysis concludes that the optimum mesh size for the femoral bone and stem is 4.5 mm and 3 mm, respectively. This phase is a critical stage that must be completed before conducting further FEA to ensure that the results are not influenced by the mesh size. However, the study presents only one approach for doing convergence analysis; it is advisable to employ many methods to guarantee that the obtained mesh size is more dependable and precise.

ACKNOWLEDGEMENT

This study was financially funded by the Universiti Teknologi Malaysia (UTM).

REFERENCES

- Abd Aziz, A. U., Ammarullah, M. I., Ng, B. W., Gan, H.-S., Abdul Kadir, M. R., & Ramlee, M. H. (2024). Unilateral external fixator and its biomechanical effects in treating different types of femoral fracture: A finite element study with experimental validated model. *Heliyon*, 10(4), e26660. <https://doi.org/10.1016/j.heliyon.2024.e26660>
- Abdullah, N. N. A., Ammarullah, M. I., Mohd Salaha, Z. F., Baharuddin, M. H., Abdul Kadir, M. R., Ramlee, M. H. (2025). Bioinspired porous hip implants design: A systematic review of mechanical testing and additive manufacturing. *Results in Engineering*, 25, 103708. <https://doi.org/10.1016/j.rineng.2024.103708>
- Alkhatib, S. E., Mehboob, H., Tarlochan, F. (2019). Finite element analysis of porous titanium alloy hip stem to evaluate the biomechanical performance during walking and stair climbing. *Journal of Bionic Engineering*, 16, 1103–1115. <https://doi.org/10.1007/s42235-019-0122-4>
- Arabnejad, S., Johnston, B., Tanzer, M., Pasini, D. (2017). Fully porous 3D printed titanium femoral stem to reduce stress-shielding following total hip arthroplasty. *Journal of Orthopaedic Research*, 35(8), 1774–1783. <https://doi.org/10.1002/jor.23445>
- Bilgi-Ozyetim, E., Dinçer, G., Sulaiman, A., Dayan, Ş. Ç., Kurtulmuş-Yılmaz, S., & Geçkili, O. (2025). Biomechanical comparison of various implant inclinations and abutment types in a bendable implant system. *BMC Oral Health*, 25(1), 1213. <https://doi.org/10.1186/s12903-025-06610-1>
- Borah, V., Bora, U., Baishya, U. J., Pegu, B., Sahai, N. (2021). Anatomization of wear behaviour of materials for total hip arthroplasty bearing surfaces: A review. *Materials Today: Proceedings*, 44(Part 1), 176–186. <https://doi.org/10.1016/j.matpr.2020.08.553>
- Cheah, Y. K., Azman, A. H., Bajuri, M. Y. (2022). Finite-element analysis of load-bearing hip implant design for additive manufacturing. *Journal of Failure Analysis and Prevention*, 22(2), 356–367. <https://doi.org/10.1007/s11668-021-01304-6>
- Chen, Y., Pani, M., Taddei, F., Mazzà, C., Li, X., Viceconti, M. (2014). Large-scale finite element analysis of human cancellous bone tissue micro computer tomography data: A convergence study. *Journal of Biomechanical Engineering*, 136(10), 101013. <https://doi.org/10.1115/1.4028106>
- Choroszyński, M., Choroszyński, M. R., Skrzypek, S. J. (2017). Biomaterials for hip implants – Important considerations relating to the choice of materials. *Bio-Algorithms and Med-Systems*, 13(3), 133–145. <https://doi.org/10.1515/bams-2017-0017>
- Cook, R. D., Malkus, D. S., Plesha, M. E., & Witt, R. J. (2002). *Concepts and Applications of Finite Element Analysis* (4th ed.). Wiley.
- De Sterck, H., Manteuffel, T., McCormick, S., Nolting, J., Ruge, J., Tang, L. (2008). Efficiency-based h- and hp-refinement strategies for finite element methods. *Numerical Linear Algebra with Applications*, 15(1), 89–114. <https://doi.org/10.1002/nla.567>
- Delikanli, Y. E., Kayacan, M. C. (2019). Design, manufacture, and fatigue analysis of lightweight hip implants. *Journal of Applied Biomaterials & Functional Materials*, 17(2). <https://doi.org/10.1177/2280800019836830>
- Fish, J., Belytschko, T. (2007). *A first course in finite elements* (eBook edition). John Wiley & Sons, Ltd. <https://doi.org/10.1002/9780470510858>
- Guzmán, M., Durazo, E., Ortiz, A., Saucedo, I., Siqueiros, M., González, L., & Jiménez, D. (2022). Finite element assessment of a hybrid proposal for hip stem, from a standardized base and different activities. *Applied Sciences*, 12(16), 7963. <https://doi.org/10.3390/app12167963>
- Gök, M. G. (2021). Creation and finite-element analysis of multi-lattice structure design in hip stem implant to reduce the stress-shielding effect. *Proceedings of the Institution of Mechanical Engineers, Part L: Journal of Materials: Design and Applications*, 236(2), 429–439. <https://doi.org/10.1177/14644207211046200>
- Jetté, S., Brailovski, V., Simoneau, C., Dumas, M., Terriault, P. (2018). Development and in vitro validation of a simplified numerical model for the design of a biomimetic femoral stem. *Journal of the Mechanical Behavior of Biomedical Materials*, 77, 539–550. <https://doi.org/10.1016/j.jmbbm.2017.10.019>
- Kim, J. T., Jung, C. H., Shen, Q. H., Cha, Y. H., Park, C. H., Yoo, J. I., Song, H. K., Jeon, Y., Won, Y. Y. (2019). Mechanical effect of different implant caput-collum-diaphyseal angles on the fracture surface after fixation of an unstable intertrochanteric fracture: A finite element analysis. *Asian Journal of Surgery*, 42(11), 947–956. <https://doi.org/10.1016/j.asjsur.2019.01.008>
- Kladovasilakis, N., Tsongas, K., Tzetzis, D. (2020). Finite element analysis of orthopedic hip implant with functionally graded bioinspired lattice structures. *Biomimetics*, 5(3), 44. <https://doi.org/10.3390/biomimetics5030044>
- Mohamad Azmi, N. A., Abdullah, N. N. A. A., Mohd Salaha, Z. F., Ramlee, M. H. (2024). Convergence study of three-dimensional upper skull model: A finite element method. In F. Hassan, N. Sunar, M. A. Mohd Basri, M. S. A. Mahmud, M. H. I. Ishak, & M. S. Mohamed Ali (Eds.), *Methods and*

- applications for modeling and simulation of complex systems. *AsiaSim 2023 (Communications in Computer and Information Science, Vol. 1912, pp. 351–361). Springer.* https://doi.org/10.1007/978-981-99-7243-2_30
- Mughal, U., Khawaja, H., Moatamedi, M. (2015). Finite element analysis of human femur bone. *The International Journal of Multiphysics*, 9(2), 101–108. <https://doi.org/10.1260/1750-9548.9.2.101>
- Prasad, K., Bazaka, O., Chua, M., Rochford, M., Fedrick, L., Spoor, J., Symes, R., Tieppo, M., Collins, C., Cao, A., Markwell, D., Ostrikov, K., Bazaka, K. (2017). Metallic biomaterials: Current challenges and opportunities. *Materials*, 10(8), 884. <https://doi.org/10.3390/ma10080884>
- Ramlee, M. H., Aziz, A. U. A., Wahab, A. A., Seng, G. H., Mohd Latip, H. F., Kadir, M. R. A. (2018). Biomechanical analysis of different material of delta external fixator for ankle joint - The effect of standing. In *2018 2nd International Conference on BioSignal Analysis, Processing and Systems (ICBAPS)* (pp. 81–86). IEEE. <https://doi.org/10.1109/ICBAPS.2018.8527420>
- Ramlee, M. H., Kadir, M. R., Murali, M. R., Kamarul, T. (2014). Biomechanical evaluation of two commonly used external fixators in the treatment of open subtalar dislocation—a finite element analysis. *Medical Engineering & Physics*, 36(10), 1358–1366. <https://doi.org/10.1016/j.medengphy.2014.07.001>
- Salaha, Z. F. M., Ammarullah, M. I., Abdullah, N. N. A. A., Aziz, A. U. A., Gan, H.-S., Abdullah, A. H., Abdul Kadir, M. R., Ramlee, M. H. (2023). Biomechanical effects of the porous structure of gyroid and Voronoi hip implants: A finite element analysis using an experimentally validated model. *Materials*, 16(9), 3298. <https://doi.org/10.3390/ma16093298>
- Shichman, I., Roof, M., Askew, N., Nherera, L., Rozell, J. C., Seyler, T. M., Schwarzkopf, R. (2023). Projections and epidemiology of primary hip and knee arthroplasty in Medicare patients to 2040–2060. *JBJS Open Access*, 8(1), e22.00112. <https://doi.org/10.2106/JBJS.OA.22.00112>
- Singh, J. A., Yu, S., Chen, L., Cleveland, J. D. (2019). Rates of total joint replacement in the United States: Future projections to 2020–2040 using the National Inpatient Sample. *The Journal of Rheumatology*, 46(9), 1134–1140. <https://doi.org/10.3899/jrheum.170990>
- Spirka, T. A., Erdemir, A., Spaulding, S. E., Yamane, A., Telfer, S., Cavanagh, P. R. (2014). Simple finite element models for use in the design of therapeutic footwear. *Journal of Biomechanics*, 47(12), 2948–2955. <https://doi.org/10.1016/j.jbiomech.2014.07.020>
- Tafreshi, O. A., Hoa, S. V., Shadmehri, F., Hoang, D. M., Rosca, D. (2019). Heat transfer analysis of automated fiber placement of thermoplastic composites using a hot gas torch. *Advanced Manufacturing: Polymer & Composites Science*, 5(4), 206–223. <https://doi.org/10.1080/20550340.2019.1686820>
- Trentadue, B., Ceddia, M., & Callea, C. (2023). Design and optimization of an artificial hip joint by finite element analysis. *Biomedical Journal of Scientific & Technical Research*, 48(1), 39132–39140. <https://doi.org/10.26717/BJSTR.2023.48.007598>
- Yaman, Y., Tunçöz, İ. O., Yang, Y., Arslan, P., Kalkan, U., Tıraş, H., Gürses, E., Şahin, M., Özgen, S. (2015). Decamber morphing concepts by using a hybrid trailing edge control surface. *Aerospace*, 2(3), 482–504. <https://doi.org/10.3390/aerospace2030482>
- Zienkiewicz, O. C., Taylor, R. L., & Zhu, J. Z. (2013). *The Finite Element Method: Its Basis and Fundamentals* (7th ed.). Butterworth-Heinemann.